Long-Distance Effects of Site-Directed Mutations on Backbone Conformation in Bacteriorhodopsin from Solid State NMR of [1-^{13}C]Val-Labeled Proteins

Michikazu Tanio,* Sayuri Inoue,* Kiyonobu Yokota,* Toshizo Seki,* Satoru Tuzi,* Richard Needleman,# Janos K. Lanyi,§ Akira Naito,* and Hazime Saitô*

*Department of Life Science, Himeji Institute of Technology, Harima Science Garden City, Kamigori, Hyogo 678-1297, Japan, #Department of Biochemistry, Wayne State University, Detroit, Michigan 48201, and §Department of Physiology and Biophysics, University of California, Irvine, California 92697-4560 USA

ABSTRACT We have recorded ^{13}C cross-polarization-magic angle spinning and dipolar decoupled-magic angle spinning NMR spectra of [1-^{13}C]Val-labeled wild-type bacteriorhodopsin (bR), and the V49A, V199A, T46V, T46V/V49A, D96N, and D85N mutants, in order to study conformational changes of the backbone caused by site-directed mutations along the extracellular surface and the cytoplasmic half channel. On the basis of spectral changes in the V49A and V199A mutants, and upon specific cleavage by chymotrypsin, we assigned the three well-resolved ^{13}C signals observed at 172.93, 172.00, and 171.11 ppm to [1-^{13}C]Val 69, Val 49, and Val 199, respectively. The local conformations of the backbone at these residues are revealed by the conformation-dependent ^{13}C chemical shifts. We find that at the ambient temperature of these measurements Val 69 is not in a β-sheet, in spite of previous observations by electron microscopy and x-ray diffraction at cryogenic temperatures, but in a flexible turn structure that undergoes conformational fluctuation. Results with the T46V mutant suggest that there is a long-distance effect on backbone conformation between Thr 46 and Val 49. From the spectra of the D85N and E204Q mutants there also appears to be coupling between Val 49 and Asp 85 and between Asp 85 and Glu 204, respectively. In addition, the T_2 measurement indicates conformational interaction between Asp 96 and extracellular surface. The protonation of Asp 85 in the photocycle therefore might induce changes in conformation or dynamics, or both, throughout the protein, from the extracellular surface to the side chain of Asp 96.

INTRODUCTION

Bacteriorhodopsin (bR) is a light-driven proton pump in the purple membrane of *Halobacterium salinarium*, in which retinal is covalently linked to Lys 216 through a protonated Schiff base (Stoeckenius and Bogomolni, 1982; Mathies et al., 1991; Lanyi, 1993, 1997; Maeda et al., 1997). Proton transport in bR is activated by photoisomerization of all-*trans* retinal to the 13-*cis* form, followed by proton transfer from the retinal Schiff base to Asp 85, release of a proton from residues or water molecule(s) at the extracellular surface, and uptake from cytoplasmic surface through reprotonation of the Schiff base by Asp 96 (Brown et al., 1994a, 1995; Yamazaki et al., 1995, 1996, 1998; Richter et al., 1996; Balashov et al., 1997; Dioumaev et al., 1998). Glu 204 is an essential part of the proton release chain, and proton release upon deprotonation of the retinal Schiff base is abolished by its replacement with glutamine (Brown et al., 1995; Govindjee et al., 1996; Rammelsberg et al., 1998). Likewise, the mutation of Glu 194 with glutamine (Dioumaev et al., 1998) or cysteine (Balashov et al., 1997) also resulted in greatly delayed proton release. It appears that the proton release group interacts with several residues and probably with water molecules. In addition, mutation of Arg 82 is known to affect the pK_a values of Asp 85 and Glu 204, as well as proton release (Govindjee et al., 1996). A water molecule between Arg 82 and Glu 204 in the recent x-ray diffraction structure (Fig. 1) is a possible candidate for the origin of the released proton (Luecke et al., 1998).

Proton uptake at the cytoplasmic side is initiated by deprotonation of Asp 96, and it has been suggested from changes in the Fourier transform infrared spectroscopy (FTIR) amide (peptide) bands in many mutants (Brown et al., 1994b; Yamazaki et al., 1995, 1996, 1998) that this may be influenced by long-range conformational interactions in the D85-V49-T46-D96 domain. In this scheme, Val 49 could play a key role in the information of protonation at Asp 85 to transfer to Asp 96 through hydrogen-bonding interaction with Thr 46 (Yamazaki et al., 1995), and its peptide C=O influences the proton acceptor function of the retinal Schiff base (Yamazaki et al., 1998). However, in the unphotolyzed state at least, the recent x-ray diffraction studies did not reveal the presence of such interactions between Val 49 and Thr 46 or between Asp 85 and Val 49, although a hydrogen bond between Asp 96 and hydroxyl group of Thr 46 was found (Pebay-Peyroula et al., 1997; Luecke et al., 1998; Essen et al., 1998). Long-distance effect on backbone conformation may become evident, however, from the three-dimensional structures of the photointermediates, either from x-ray diffraction or cryo-electron microscopy (Henderson et al., 1990; Grigorieff et al., 1996; Kimura et al., 1997). Such effect may be a common mech-

Received for publication 26 January 1999 and in final form 13 April 1999.

Address reprint requests to Dr. Hazime Saitô, Department of Life Science, Himeji Institute of Technology, Harima Science Garden City, Kamigori, Hyogo 678-1297, Japan. Tel.: 81-7915-8-0181, Fax: 81-7915-8-0182; E-mail: saito@sci.himeji-tech.ac.jp.

0006-3495/99/07/431/12 $2.00

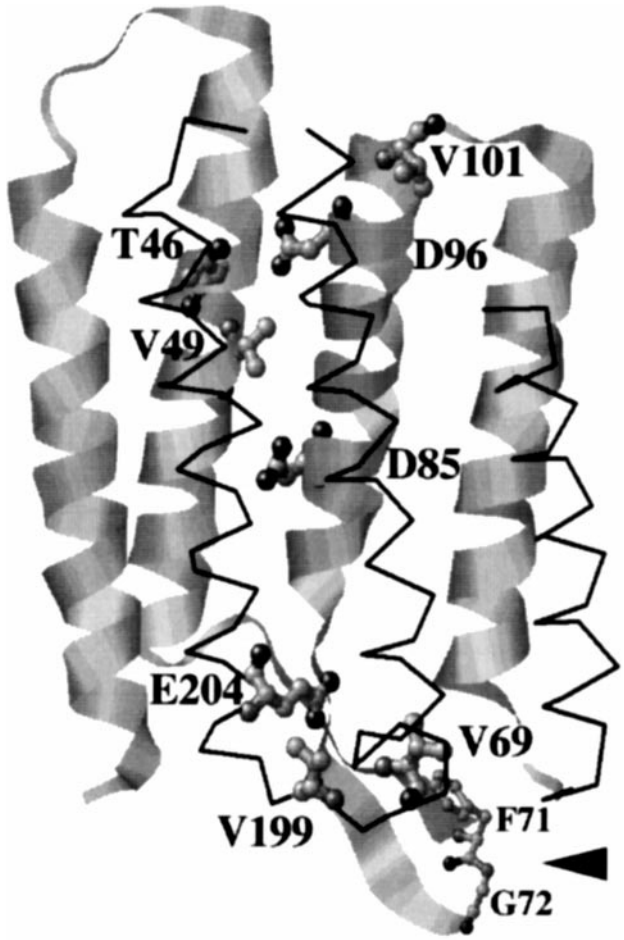

FIGURE 1 Illustration of amino acid residues relevant to the present study, from the recent 3-D structure (PDB coordinates: 1brx) by x-ray diffraction (Luecke et al., 1998). The site for cleavage by chymotrypsin is designated by the arrow.

anism in ion pumps. Bacteriorhodopsin was recently compared with cytochrome c oxidase from this point of view (Wikström, 1998).

We have demonstrated that ^{13}C NMR studies of [3-^{13}C]Ala-labeled bR provide excellent means to probe the conformation and the dynamics of the peptide backbone at ambient temperature(Tuzi et al., 1993, 1994, 1996a,b, 1999; Yamaguchi et al., 1998; Tanio et al., 1998). This is because the conformation dependence of the ^{13}C chemical shifts can be derived from model polypeptides and they vary very sensitively with the local conformation (up to 8 ppm) (Saitô, 1986; Saitô and Ando, 1989; Saitô et al., 1998). This approach proved to be especially useful for revealing local conformations and dynamics of residues at loops, or at the protruding N- or C-terminus tails (Tuzi et al., 1999; Yamaguchi et al., 1998; Tanio et al., 1998) in membrane proteins. The ^{13}C chemical shift is a valuable intrinsic probe for the movements of the transmembrane helices because dynamic structural data for these regions are not available from diffraction. In this connection, we emphasize that, in spite of their locations at the side-chain, the ^{13}C NMR signals of C_β carbons at any amino acid residue give rise to signals that reveal the local backbone conformation of the residue under consideration, when evaluated together with data for C_α and carbonyl carbons (Saitô, 1986; Saitô and Ando, 1989; Saitô et al., 1998). Thus, although we have often measured NMR spectra of ^{13}C-labeled Ala, it has been possible to utilize probes other than Ala in studies of conformation and dynamics at locations where Ala residues are not involved.

Very little data are currently available from ^{13}C NMR studies on amino acid-labeled carbons, such as [1-^{13}C]Ala, -Val, or -Leu-labeled bR, for probing the ^{13}C-labeled backbone directly (Tuzi et al., 1994, 1999; Hu et al., 1998), even though the carbonyl ^{13}C chemical shifts are intrinsically sensitive to the configuration of interchain hydrogen bonds. In addition to using [4-^{13}C]Asp-bR (Engelhard et al., 1989; Metz et al., 1992a,b) and [3- or 4-^{13}C]Pro-bR (Engelhard et al., 1996), it is therefore worthwhile to compare the ^{13}C NMR spectra of [1-^{13}C]Val-labeled wild-type and its site-specific mutant of bR, in order to detect and gain insights into the molecular mechanism of the proposed long-distance effect on backbone conformation from Asp 85 to cytoplasmic half channel and extracellular surface. In this regard, we have begun assignment of several well-resolved peaks, and identified the highest carbonyl peak of Val-labeled bR at 171.11 ppm as originating from Val 199 at the F-G loop (Tuzi et al., 1999) by utilizing the site-directed mutant V199A. Here we report additional and independent evidence, from the chemical shifts of the ^{13}C in peptide C=O groups in [1-^{13}C]Val-labeled bR and mutants, for long-distance effect on backbone conformation suggested from FTIR (Yamazaki et al., 1995, 1996, 1998).

MATERIALS AND METHODS

Sample preparation

[1-^{13}C]Valine and [3-^{13}C]Alanine were purchased from CIL, (Andover, MA) and used without purification. *H. salinarium* S-9 (wild-type), V49A, V199A, T46V, T46V/V49A, D96N, and D85N were grown in TS medium of Onishi et al. (1965), in which unlabeled L-valine or alanine was replaced by [1-^{13}C]Val or [3-^{13}C]Ala, respectively. Purple membranes from these sources were isolated by the method of Oesterhelt and Stoeckenius (1974) and concentrated by centrifugation at 39,800 $\times$ *g* for 1.5 h, followed by suspension in 5 mM HEPES buffer containing 10 mM NaCl and 0.025% (w/v) NaN_3 (pH 7.0). For the assignment of Val 69 signal, [1-^{13}C]Val-bR of wild-type was first bleached with 0.5 M NH_2OH (Tuzi et al., 1996b) and then cleaved by incubation with chymotrypsin (0.1–10 mg bR) for 2.5 h (Popot et al., 1987). The resulting cleaved bacterio-opsin (bO) was regenerated by incubation for 1.5 h at ambient temperature with retinal (1.1:1 mole bO) to yield bR, followed by centrifugation (Tuzi et al., 1996b). Samples thus prepared were placed into a 5-mm o.d. zirconia pencil-type rotor for magic angle spinning, and tightly sealed with Teflon caps glued with rapid Araldyte to prevent leakage or evaporation of water during spinning. Absorption spectra of these preparations were measured on a Shimadzu UV 2200 UV/Visible spectrophotometer (Kyoto, Japan).

Measurements of ^{13}C NMR spectra

High-resolution solid-state ^{13}C NMR spectra (100.6 MHz) were recorded on a Chemagnetics CMX-400 spectrometer by cross-polarization-magic angle spinning (CP-MAS) and dipolar decoupled-magic angle spinning

(DD-MAS) with single-pulse excitation. All measurements were performed at 20°C, unless otherwise mentioned, under dark conditions. The spectral width was 40 kHz and contact time for the CP-MAS experiment was 1 ms. Repetition time was 4 s and 4–6 s for the CP- and DD-MAS experiments, respectively. Free-induction decay of improved spectral resolution was acquired with 2K data points and Fourier-transformed as 16K after 14K data points were zero-filled. Free-induction decays of some spectra were acquired with data points of lK and Fourier-transformed either as 16K or 8K after 15K or 7K points, respectively, were zero-filled. The $\pi/2$ pulses for carbon and proton were 4.5–5 μs and the spinning rate was 2.6–4.0 kHz. Spectral deconvolution was performed by PeakFit for Windows by SPSS (Chicago, IL).

^{13}C spin-lattice relaxation times T_1 in the laboratory frame were recorded by either standard inversion recovery method based on DD-MAS or by the procedure of cross-polarization enhancement with inversion of spin temperature based on CP-MAS (Torchia, 1978). ^{13}C spin-spin relaxation times T_2 under the condition of magic angle spinning and proton irradiation were measured using a Hahn spin echo pulse sequence by adjusting the interval between π pulse and the starting point of acquisition to be multiples of the rotor period N_cT_r (Naito et al., 1998), in the usual manner.

$$M(2N_cT_r) = M(0)\exp(-2N_cT_r/T_2) \quad (1)$$

where N_c is the number of rotor periods and $M(0)$ and $M(2N_cT_r)$ are the peak intensities at the initial and interval, respectively. ^{13}C-resolved proton spin-lattice relaxation times in the rotating frame ($T_{1\rho}$) and cross-polarization times (T_{CH}) were measured by analysis of cross-polarization dynamics by measuring the peak intensities as a function of contact times. ^{13}C chemical shifts were referred to the carboxyl signal of glycine (176.03 ppm from tetramethylsilane), and then expressed as shifts relative to the value of tetramethylsilane.

RESULTS

Assignment of [1-^{13}C]Val-bR signals from the site-directed mutants, V49A and V199A, and cleavage by chymotrypsin

Fig. 2 shows ^{13}C CP-MAS (*top*) and DD-MAS NMR (*bottom*) spectra of [1-^{13}C]Val-labeled bR. At least eight peaks were resolved from the ^{13}C CP-MAS NMR spectrum, except for the presence of a small bump (*hatched peak*) arising from the background signals of natural abundance, which is

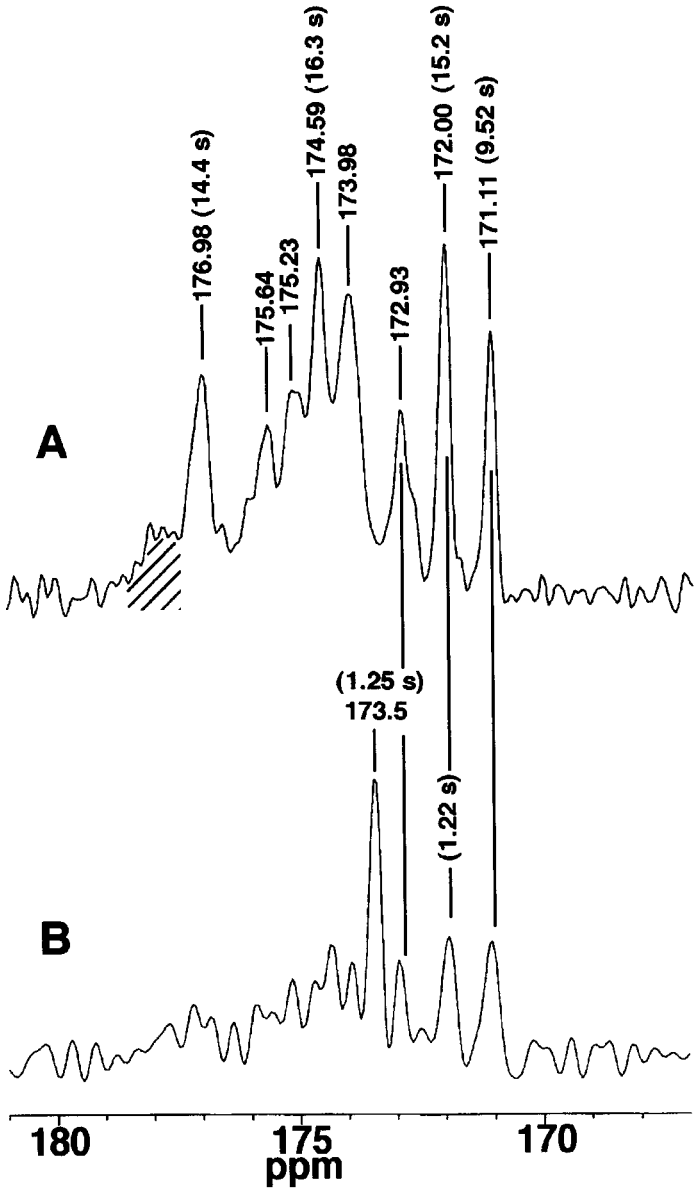

FIGURE 2 ^{13}C CP-MAS NMR (*top*) and DD-MAS NMR (*bottom*) spectra of [1-^{13}C]Val-labeled bacteriorhodopsin. The bump at the lowest chemical shift region, marked by hatching, arose from background signal. Spin-lattice relaxation times (T_1) are shown at the tops of peaks.

more pronounced in mutants such as D85N, as will be described below. The longer spin-lattice relaxation times in the CP-MAS experiments (14–16 s) indicated on the individual peaks in Fig. 2 are characteristic of rigid carbons in transmembrane helices. Surprisingly, no signal is visible in the CP-MAS NMR spectrum that would correspond to the most intense signal, at 173.5 ppm, in the DD-MAS NMR spectrum. It is probable that this peak may be ascribed to a carbonyl carbon in a Val residue located at a more flexible chain, as judged from the spin-lattice relaxation time that is one order of magnitude shorter (1.25 s) than that of the transmembrane helices. In contrast, the high-field three peaks, 171.11, 172.00, and 172.93 ppm, in the DD-MAS NMR spectrum resonated at the same positions as in the CP-MAS spectrum, although the peak intensity of the 172.00-ppm peak is substantially reduced to a value comparable to those of the other two peaks. The peaks that resonated lower than 173.98 ppm are virtually completely suppressed. This is consistent with the idea that the three high-field peaks arise from Val residues located at loops, and all other signals from transmembrane helices, including that from Val 49 superimposed on the 172.00-ppm peak to be described later, are suppressed in the DD-MAS spectrum because of their prolonged spin-lattice relaxation times. It is emphasized that this peak is composed of two components with different spin-lattice relaxation times as recorded by the CP-MAS and DD-MAS NMR spectra (Fig. 2). The peak at 171.11 ppm was previously ascribed to Val 199 (Tuzi et al., 1999).

Fig. 3 contains ^{13}C CP-MAS (*left traces*) and DD-MAS (*right traces*) NMR spectra of [1-^{13}C]Val-labeled mutants, V49A (*A*) and V199A (*B* and *D*), together with those of the wild-type as reference (*C* and *E*). It is straightforward to assign the 172.00-ppm peak to Val 49, because this peak intensity is obviously much lower in the V49A mutant than in the wild-type. We confirm that the peak at 171.1l ppm is assigned to the Val 199 signal, because this peak disappears in the ^{13}C DD-MAS NMR spectrum of V199A mutant (*trace D*). It should be emphasized that this approach for the peak assignment is feasible only when no appreciable conformational change is induced in the site-directed mutants. This is the case here, because the ^{13}C chemical shifts, which would be intrinsically sensitive to any kind of conformational changes (Saitô, 1986; Saitô and Ando, 1989; Saitô et al., 1998), are unchanged. At first glance, the local conformation at Val 49 and Val 199 would be ascribed to a β-sheet on the basis of the ^{13}C chemical shift of 171.8 ppm in [1-^{13}C]Val-labeled poly(L-valine) in β-sheet in the solid state (Saitô, 1986; Saitô and Ando, 1989; Saitô et al., 1998). This assignment is not justified for Val 49 and Val 199, however, because both are followed by a Pro residue (as is Val 69, see below), and the carbonyl ^{13}C chemical shifts of amino acid residues in such circumstances are usually displaced upfield by 1.4–2.5 ppm (Torchia and Lyerla, 1974;

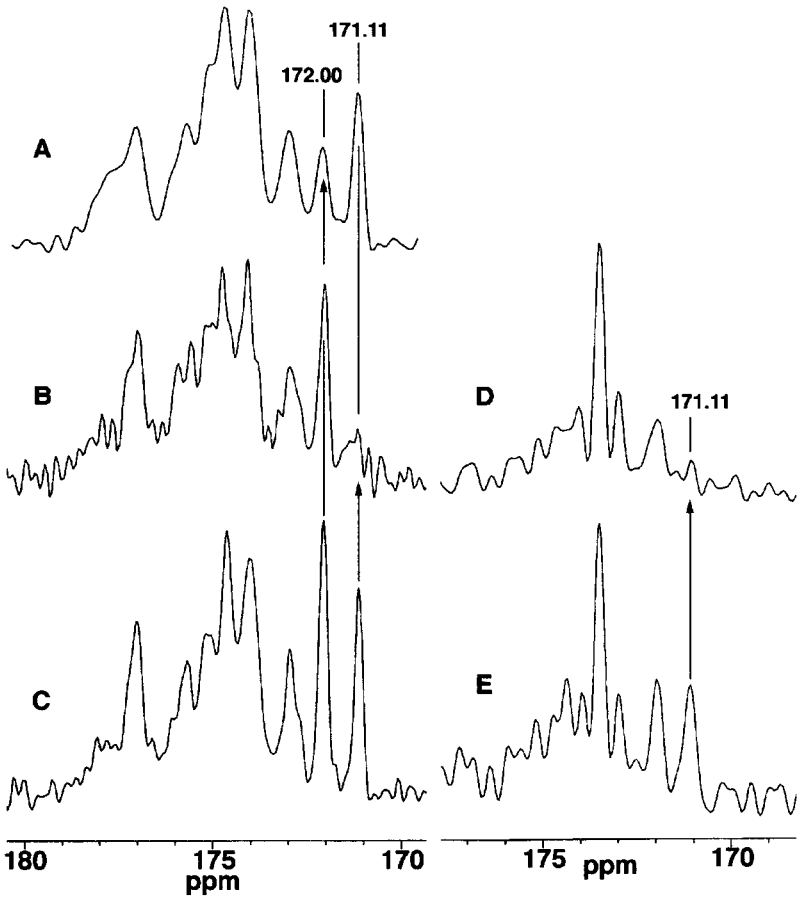

FIGURE 3 ^{13}C CP-MAS NMR spectra (*left*) and DD-MAS NMR spectra (*right*) of [1-^{13}C]Val-labeled V49 (*A*) and V199A mutants (*B* and *D*) as compared with those of wild-type (*C* and *E*).

Wishart et al., 1995). Accordingly, the corrected ^{13}C shift of Val 199 and Val 49 turned out to be 172.5–173.6 and 173.4–174.5 ppm, respectively. Peaks that resonate between 172 and 173 ppm should be ascribed to carbons at loop regions in view of the analogous assignment of peaks for [1-^{13}C]Ala-bR (Yamaguchi et al., 1998). This means that the local conformation of Val 199 and 49 are ascribed to loop and α-helix, 174.9 ppm from poly(L-valine) (Saitô, 1986; Saitô and Ando, 1989; Saitô et al., 1998), respectively. This is consistent with the x-ray diffraction structure measured at cryogenic temperatures (Kimura et al., 1997; Luecke et al., 1998; Essen et al., 1998).

In order to confirm the local conformation of Val 49 as α-helix, the conformation-dependent ^{13}C chemical shifts of C_α or C_β carbons should be determined also, as these atoms are free from effects from a neighboring Pro. In such an experiment, we compared the ^{13}C NMR spectrum of [3-^{13}C]Ala-labeled V49A mutant (*A*) with that of wild-type (*B*), as shown in Fig. 4. Indeed, we find that the ^{13}C chemical shift of the newly emerged [3-^{13}C]Ala signal for V49A (Ala 49) (*shaded peak*) in the deconvoluted spectrum (C) resonates at 16.7 ppm; that is characteristic of the α-helix (Saitô and Ando, 1989; Saitô et al., 1998). As for [1-^{13}C]Val-labeling, it is unlikely that the two peaks mentioned above for Val 49 and 199 arose from a single carbon in view of their relative peak intensities (Figs. 2 and 3), although the former peak from the transmembrane α-helix is resonated at the peak region of the loop region because of the aforementioned proline effect. In fact, it is probable that they are composite peaks, being superimposed by chance on the carbonyl carbon(s) of another Val residue located in loop regions (Val 34 in A-B loop, Val 101 in C-D, and Val 130 in D-E loop, for instance). Alternatively, they might be background signals from natural abundance, because V49A and V199A exhibit recognizable residual peaks at 172.00 and 171.11 ppm, respectively. It is therefore likely that either Val 34 or Val 130, or both, are superimposed on the peak of Val 49. This is suggested by the relaxation data for Val 199, described below. The assignment of the Val 101 peak will be also given below.

In Fig. 5, we compare the ^{13}C NMR spectra of [1-^{13}C]Val-labeled regenerated bR (*left*) and chymotrypsin-cleaved preparation (*right*) at various temperatures, for the sake of assigning the Val 69 signal. Surprisingly, the single peak at 172.9 ppm arising from two or three components that are accidentally superimposed on the uncleaved bR at 20°C is split into a doublet peak at both elevated (30°C) and low temperatures (0°C) (*left traces*). This is obviously caused by the facts that this peak consists of two Val residues and one of the peaks (172.7 ppm at 30°C, *arrow*) was suppressed in the temperature range around 20°C, and at higher temperatures displaced downfield (173.0 ppm at 0°C, *arrow*) by 0.3 ppm. This temperature effect was removed after the protein was cleaved at residues 71–72 by chymotrypsin (*right traces*). For this reason, it is probable that this carbonyl carbon is ascribed to a Val residue located at a loop region and is able to undergo conformational fluctuation with the frequency of 10^4-10^5 Hz that interferes with the proton decoupling frequency (Suwelack et al., 1980; Rothwell and Waugh, 1981). The peak intensity of this residue is not affected by temperature in the case of the chymotrypsin-cleaved preparation (*right traces*), because

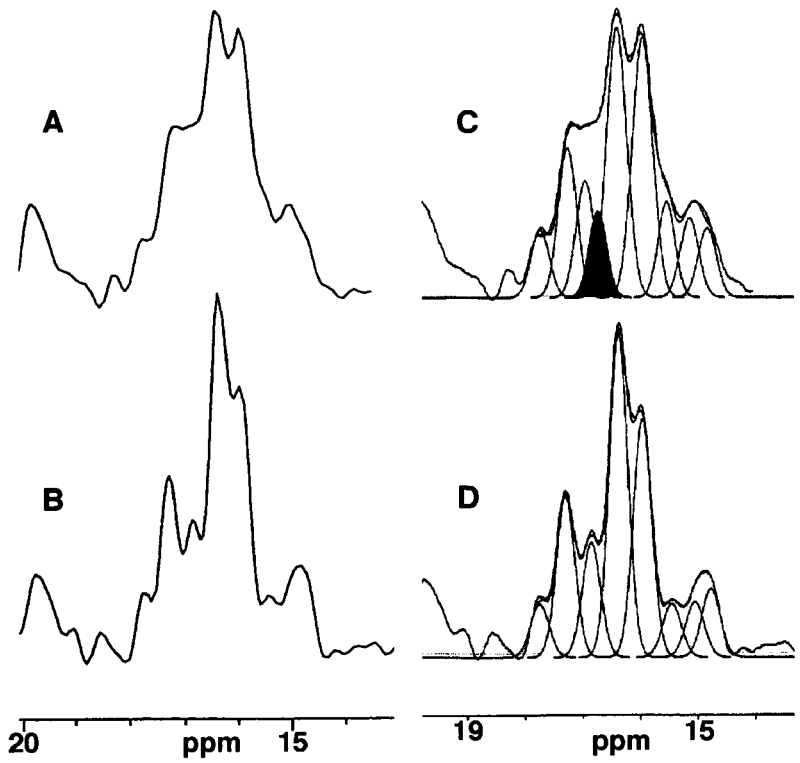

FIGURE 4 ^{13}C CP-MAS NMR of [3-^{13}C]Ala-labeled V49A (*A*) and wild-type bR (*B*). Corresponding deconvoluted spectra are shown in (*C*) and (*D*), respectively. The shaded peak in Fig. 3 *C* is the newly emerged Ala peak in the mutant.

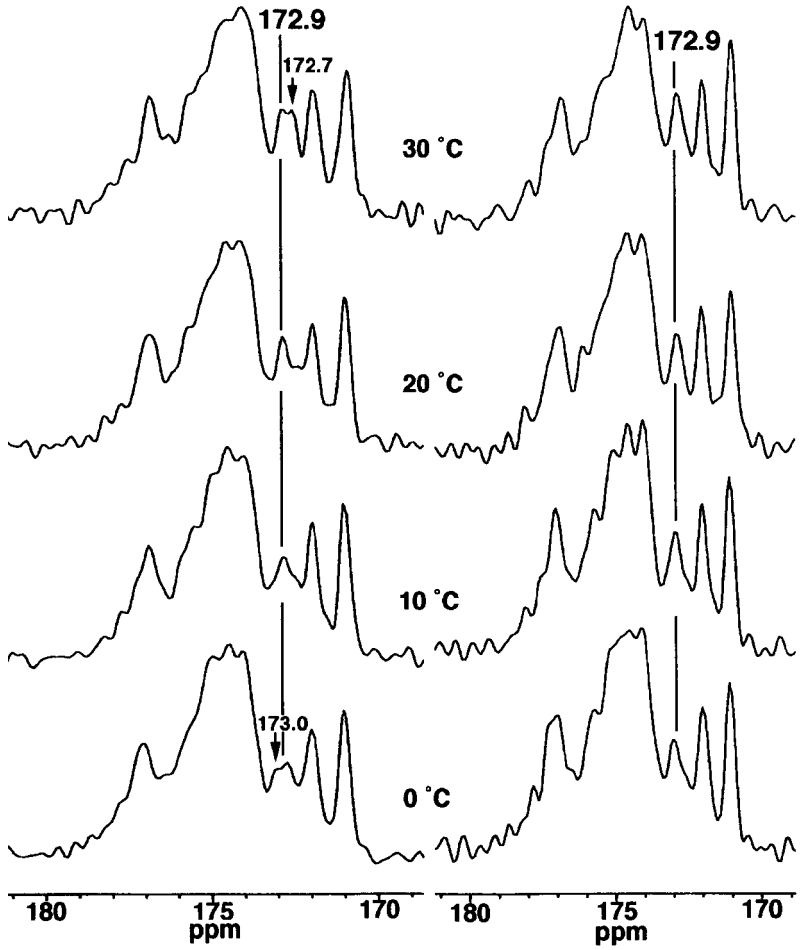

FIGURE 5 Temperature variation of ^{13}C NMR spectra of [1-^{13}C]Val-labeled regenerated bR (*left traces*) and chymotrypsin-cleaved preparation (*right*). The peak at 172.7 ppm at 30°C is shifted downfield, suppressed at 20 and 10°C, and reappears at a lower field at 0°C (*traces at left side*).

frequency for this motion would be shifted away from the proton decoupling frequency by this treatment. Therefore, the peak at 172.9 ppm was assigned to Val 69, which is the only Val residue near the chymotrypsin cleavage-site (in the B-C interhelical loop). When corrected downfield by 1.4–2.5 ppm to 174.3–175.4 ppm because Pro 70 follows it, the local conformation of the peptide bond at Val 69 is thus far from what one would expect if the B-C interhelical loop were in the β-sheet (171.8 ppm), as in the structures described from cryo-electron microscopy or low temperature x-ray diffraction (Kimura et al., 1997; Luecke et al., 1998; Essen et al., 1998). Instead, we conclude that at ambient temperature the backbone at this residue adopts a flexible turn structure, undergoing rapid reorientational motion as judged from the spectral observation by the DD-MAS experiment (Fig. 2 *B*). Indeed, it appears that the carbonyl ^{13}C chemical shifts of amino acid residues taking random coil conformation is rather close to those of α-helix form (Howarth and Lilley, 1978; Wishart et al., 1991; Yamaguchi et al., 1998).

Changes in the local backbone conformation and dynamics due to site-directed mutagenesis

Fig. 6 shows ^{13}C CP-MAS NMR spectra in whole carbonyl region (left), and in an expanded region that includes the loop region only (*right*), of the [1-^{13}C]Val-labeled mutants D96N, T46V, and T46V/V49A. Naturally, the shoulder peak denoted with an arrow at 177.5 ppm in the T46V and T46V/V49A mutants can be ascribed to the new Val 46 signal. The assignment of the 172.15 ppm peak to Val 49 in the presence of the T46V mutation is confirmed by its disappearance in the T46V/V49A double mutant. The most notable spectral change is that the accidentally overlapped Val 69 signal of wild-type at 172.93 ppm is split into the two peaks at 172.76 and 173.52 ppm, in view of the relative peak intensities, in the D96N mutant. The former peak position (172.76 ppm) is the same as that of Val 69 signal in wild-type (Fig. 5) and the latter (173.52 ppm) is straightforwardly ascribed to the shifted peak from the peak at 172.93 ppm of Val 101 (Fig. 1) in this mutant, because this Val residue, and no other, is close to Asp 96 (Henderson et al., 1990; Grigorieff et al., 1996; Pebay-Peyroula et al., 1997; Kimura et al., 1997; Luecke et al., 1998; Essen et al., 1998). It is also noteworthy that there appears a slight downfield displacement of the peak for Val 49 in the T46V mutant, by 0.15 ppm (as compared with the digital resolution 0.025 ppm in this case), even though the other peaks are nearly unchanged.

Fig. 7 shows the ^{13}C CP-MAS NMR spectra of [1-^{13}C]Val-labeled D85N (*B*) and E204Q (*C*), together with the spectrum of the wild-type (*A*). As in Fig. 6, they are

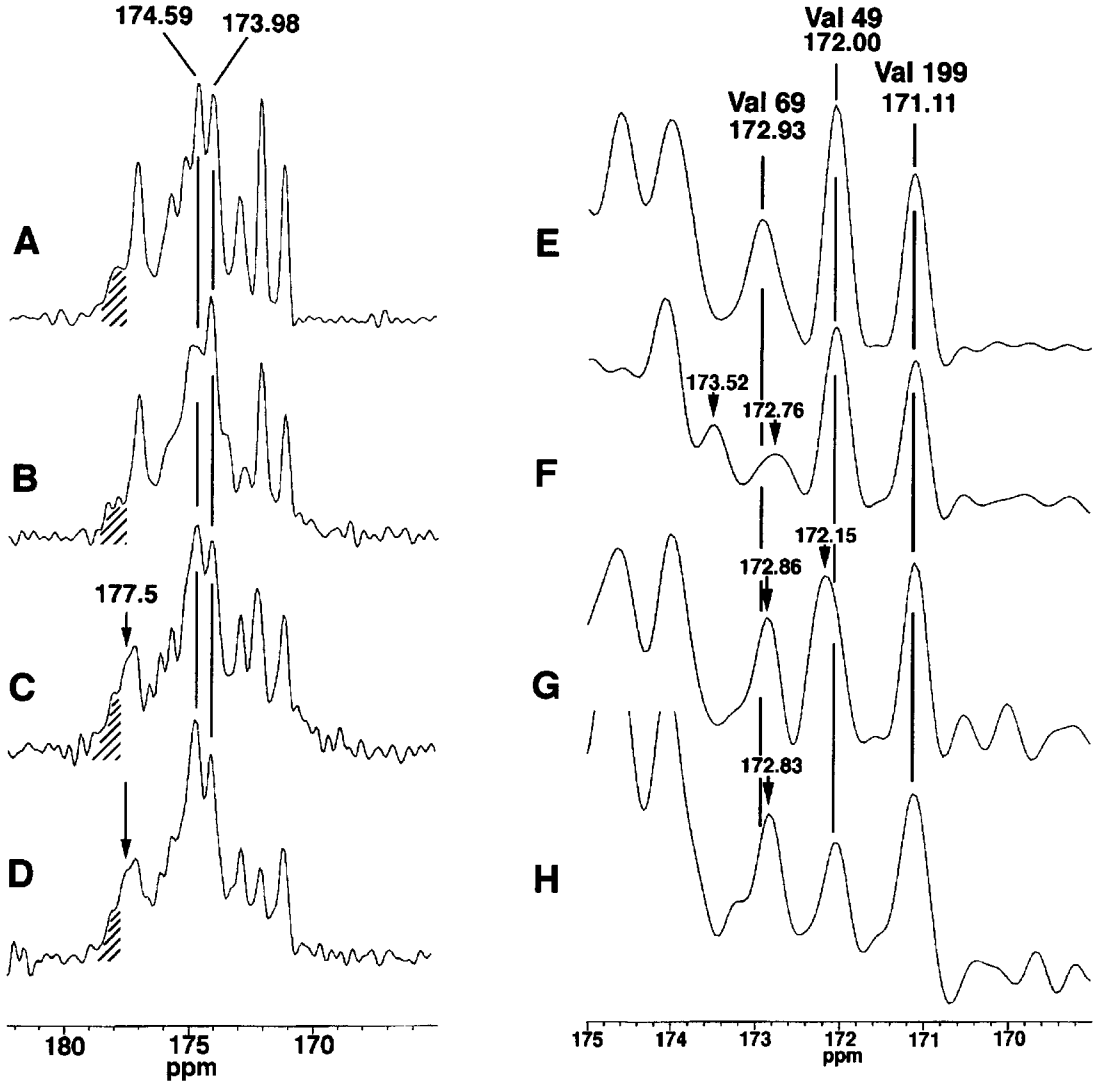

FIGURE 6 ^{13}C NMR spectra of [1-^{13}C]Val-labeled wild-type (*A*), D96N (*B*), T46V (*C*), and T46V/V49A (*D*) mutants. The lowest peaks in (*C*) and (*D*), indicated by the arrows, can be ascribed to the new residue Val 46. The traces at the right side (*E-H*) are expanded spectra corresponding to the spectra (*A-D*) for the range 170–175 ppm.

shown as expanded traces on the right side. The most prominent spectral changes are noted for D85N mutant, both from the peak intensities and spectral features especially at the transmembrane helices at the lower field region. As to the former, the peak intensities from transmembrane helices, including the signal from Val 49, seem to be reduced when compared with those of the hatched peaks from the background signals. As to the latter, the two peaks at 176.98 and 174.49 ppm of the wild-type are displaced upfield and downfield by 2.0 and 0.37 ppm, respectively, and merged to the peak at 174.98 ppm. It is probable that such drastic displacements of the carbonyl peaks must be interpreted in terms of a large-scale conformational change that includes modification of the local torsion angles or hydrogen bonding, or both. However, in projection, and at a 7-Å resolution, the structure of D85N appeared similar to the wild-type (Kataoka et al., 1993). More importantly in relation to the question of long-distance effect, the Val 49 signal of D85N is displaced either downfield by 0.28 ppm or upfield by 0.12 ppm with respect to that of the wild-type (172.00 ppm). In contrast, the Val 49 signal is displaced upfield by 0.05 ppm (although this shift is only slightly larger than the digital resolution, at 0.025 ppm) in E204Q. The Val 69 peak for D85N and E204Q is split into double or triple peaks, as in D96N, although no further spectral change was noted in the latter mutant.

We have evaluated ^{13}C spin-spin relaxation times for wild-type and a variety of mutants under the condition of cross-polarization magic-angle spinning and high-power proton decoupling (T_2) (Suwelack et al., 1980; Rothwell and Waugh, 1981), from the slope of a linear plot of the relative peak intensity versus interval between the contact and π pulse, as shown in Fig. 8 for Val 199. The results are summarized in Table 1. We expected that the transverse

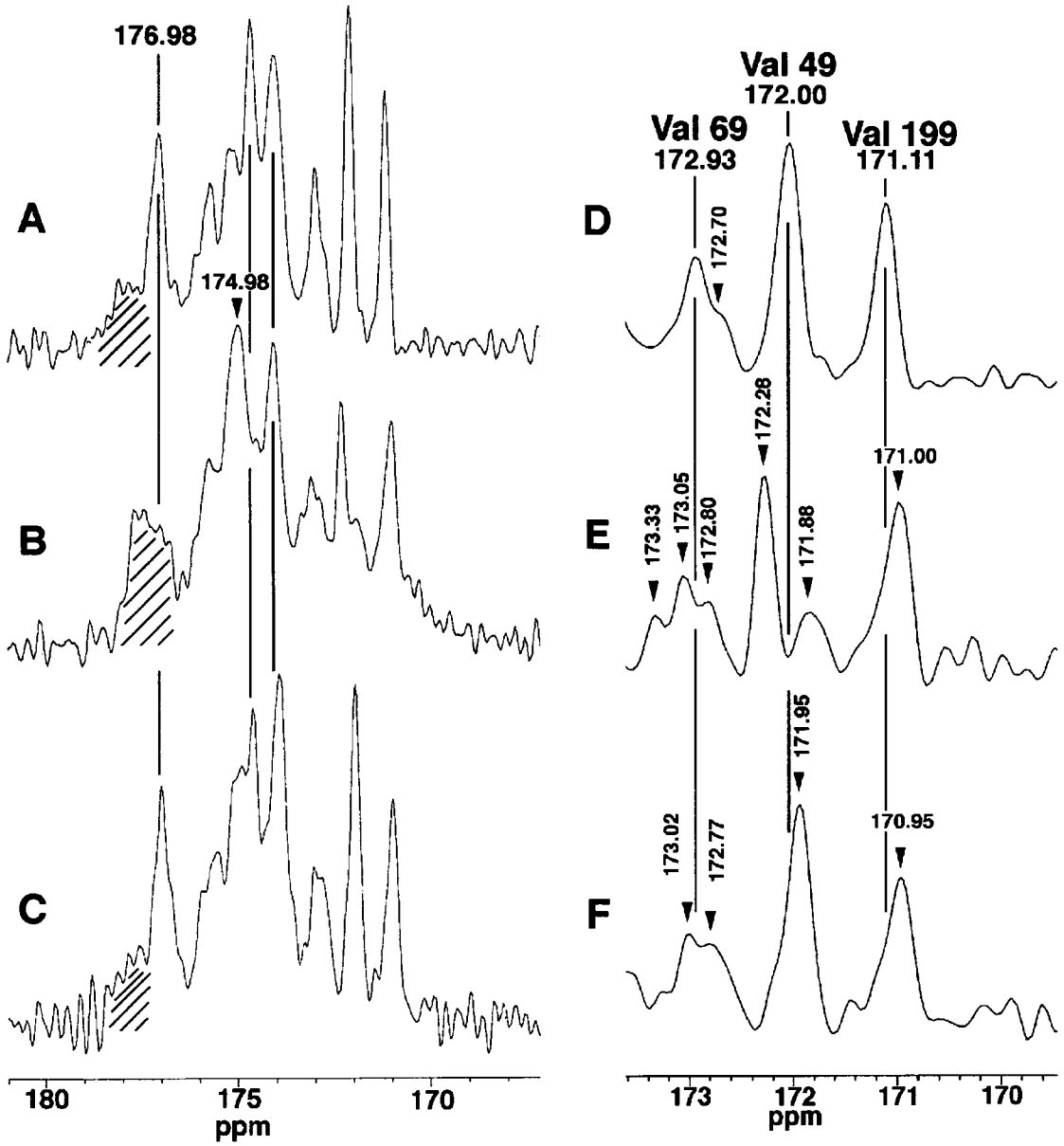

FIGURE 7 ^{13}C NMR spectra of [1-^{13}C]Val-labeled D85N (*B*) and E204Q (*C*) mutants as compared with wild-type (*A*). The hatched bump at the lowest chemical shift region is ascribed to a background signal. The traces (*D-F*) on the right side are expanded spectra for the region of 170–173 ppm.

magnetization of the carbonyl carbons would be sensitive to the backbone dynamics of the respective carbon close to the rate of magic angle spinning (10^4 Hz), because it decays mainly via fluctuation of chemical shift interaction (Suwelack et al., 1980; Rothwell and Waugh, 1981), as shown in Eq. 2:

$$1/T_2 = \omega_0^2\delta^2\eta^2/45(\tau_c/(1 + 4\omega_r^2\tau_c^2) + 2\tau_c/(1 + \omega_r^2\tau_c^2)) \qquad (2)$$

where ω_o and ω_r are the carbon resonance frequency and the rotor frequency, respectively, and τ_c, δ, and η are the correlation time of conformational fluctuation, chemical shift anisotropy, and its asymmetry parameter, respectively.

Interestingly, the T_2 value for Val 199 of wild-type takes the greatest value at 14 ms, in contrast to 5–7 ms in the transmembrane region. The peak of Val 49, however, assumes an intermediate value, apparently the result of superimposition of the contributions from the shorter value of the transmembrane helix and the seemingly longer value of the superimposed peak in the loop. It is not clear why they are averaged and do not assume distinct T_2 values. They should be considered as effective T_2, consisting of two contributions. The ^{13}C-resolved proton spin-lattice relaxation times in the rotating frame ($T_{1\rho}$) and cross-polarization times (T_{CH}) are also summarized in Table 1. There appears to be no significant variation of the several types of carbon-resolved proton spin-lattice relaxation times among wild-type and mutants. This may be because a rapid spin diffusion process allows all the relaxation parameters to become

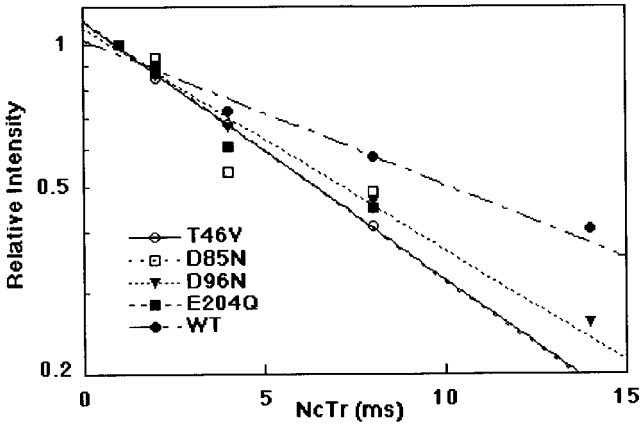

FIGURE 8 Plot of the relative peak intensities for the Val 199 signal against the interval between π pulses. The symbols for a variety of mutants and wild-type are indicated in the figure.

identical unless a portion undergoes conformational fluctuation, as demonstrated earlier for [3-^{13}C]Ala-labeled bR and bO (Tuzi et al., 1996b).

DISCUSSISON

Conformation and backbone dynamics

At ambient temperature, eight well-resolved ^{13}C NMR peaks were observed for [1-^{13}C]Val-labeled bR (Fig. 2). They originate from the 18 Val residues and their displacements are spread between 171 and 177 ppm, depending upon the local backbone secondary structure. We were able to assign the carbonyl signals of Val 199, Val 49, Val 69, and Val 101, even though none the peaks arose from single carbon atom but overlapped with at least one other peak. Nevertheless, these peaks are useful as intrinsic probes for examining the backbone conformation, as revealed by conformation-dependent chemical shifts (Saitô, 1986; Saitô and Ando, 1989; Saitô et al., 1998), in [1-^{13}C]Val-labeled wild-type and mutant bRs. For example, we found that the Val 101 signal overlaps with Val 69 signal in wild-type but becomes separated from it at temperatures above or below 20°C or in the D96N mutant.

If a Val residue is followed by a Pro residue, as in the case of Val 49, Val 69, and Val 199, a correction to the observed ^{13}C chemical shift for the proline effect of up to 2.6 ppm (Torchia and Lyerla, 1974; Wishart et al., 1995) is essential for assessing the backbone conformation from the carbonyl ^{13}C chemical shifts. As a result, we found that [1-^{13}C]Val 49 that resonated at 172.00 ppm is ascribed to an α-helix region in spite of its raw chemical shift data that would be otherwise characteristic of a β-sheet conformation. This assignment was confirmed on the basis of the conformation-dependent ^{13}C chemical shift of [3-^{13}C]Ala-labeled mutant, V49A (Fig. 4) and is consistent with the 3-D crystal structure (Henderson et al., 1990; Grigorieff et al., 1996; Pebay-Peyroula et al., 1997; Kimura et al., 1997; Luecke et al., 1998; Essen et al., 1998). Interestingly, the [1-^{13}C]Val 49 chemical shift is very close to that in the synthetic fragment B of bR incorporated into DMPC bilayer, 172.8 ppm (S. Kimura, A. Naito, and H. Saitô, manuscript in preparation). Proton NMR of a bO segment that included residues from 1 to 71 indicated that the region around Val 49 is α-helical (Pervushin et. al., 1994). The significant difference (0.8 ppm) in the chemical shift between the intact protein and its fragment can be ascribed to the presence or absence of interchain interactions. One candidate for such interaction may be Asp 85, because the Val 49 peak position was modified in the D85N mutant.

It is interesting to note that Val 69 is not involved in a rigid extracellular β-sheet, at least at the ambient temperature of our measurements. We conclude this from both the conformation-dependent ^{13}C chemical shift and the backbone dynamics, which exhibits motions with a correlation time of 10^{-5} s and interferes with the proton decoupling frequency (Fig. 5). This contrasts with the structure based on cryo-electron microscopy (Kimura et al., 1997) or low-temperature x-ray diffraction (Pebay-Peyroula et al., 1997; Luecke et al., 1998; Essen et al., 1998). This contradiction is undoubtedly due to the fact that backbone dynamics at the B-C loop (but not in the intrahelical region near Val 49, see above) are strongly dependent on temperature.

Comparison of the CP-MAS and DD-MAS NMR spectra based on differential T_1 value was very useful for distinguishing the Val 49 signal from the unassigned peak at 172.00 ppm, as demonstrated in Fig. 2. This is because correlation time of acquired motional freedom on the time scale of 10^{-8} s in the loop region shortened the T_1 values as compared with those at the transmembrane helices. In a similar manner, it is probable that the rather longer T_2 value of Val 49, 9.5 ms, as compared with that of other transmembrane helices, 5–7 ms, arises from the superimposed signal in the loop region, although this correlation time is in the order of 10^{-4} s. This may be caused by heterogeneity in the correlation times, which are sensitive to fast or slow molecular motions, provided that the motions are highly anisotropic.

The most significant displacement of peaks due to site-directed mutagenesis is noted for the carbonyl peak in the transmembrane α-helix of D85N (174.98 ppm) by the amount of 2.0 ppm rather than that in the loop region, probably due to the presence of accompanying distortion in hydrogen bonds, in addition to a change in the torsion angles in the α-helical region as a result of relatively large-scale conformational changes. This view is supported by the observation of shortened spin-lattice relaxation (Fig. 2) and spin-spin relaxation times of CP-MAS experiment (Table 1), especially for Val 199 of the wild-type. Therefore, it is likely that the displacement of the ^{13}C chemical shift of Val 199 in the F-G loop in D85N is less pronounced (0.11 ppm) because of intrinsic conformational fluctuation, as mentioned already, as compared with the peaks from the transmembrane helices (2.00 ppm).

TABLE 1 ^{13}C T_2, T_{CH}, and $T_{1\rho}$ of [1-^{13}C]Val-labeled bR (ms)

		Loop		Transmembrane helix			
		Val 199 (171.11 ppm)	Val 69 (172.98 ppm)	Val 49 (172.00 ppm)	174.1 ppm	174.7 ppm	175.0 ppm
wild-type	T_2	14.1 ± 1.0	6.3 ± 0.7	9.5 ± 0.5	6.9 ± 0.4	5.7 ± 0.4	
	T_{CH}	0.4 ± 0.06	0.4 ± 0.05	0.5 ± 0.02	0.3 ± 0.04	0.3 ± 0.01	
	$T_{1\rho}$	4.5 ± 0.6	4.8 ± 0.7	6.2 ± 0.3	5.4 ± 0.6	5.0 ± 0.01	
T46V	T_2	8.0 ± 0.3	5.4 ± 0.7	8.4 ± 0.6	5.8 ± 0.4	5.7 ± 0.4	
	T_{CH}	0.3 ± 0.02	0.3 ± 0.02	0.3 ± 0.02	0.3 ± 0.03	0.4 ± 0.02	
	$T_{1\rho}$	5.5 ± 0.3	5.3 ± 0.4	5.4 ± 0.4	5.4 ± 0.5	6.0 ± 0.4	
D85N	T_2	7.8 ± 2.6	4.4 ± 0.9	10.8 ± 2.6	5.0 ± 0.4		5.7 ± 1.2
	T_{CH}	0.5 ± 0.06		0.6 ± 0.3			0.4 ± 0.05
	$T_{1\rho}$	13.1 ± 3.4		7.5 ± 5.3	4.4 ± 0.3		7.0 ± 1.2
D96N	T_2	9.2 ± 0.6	5.8 ± 1.1	10.0 ± 0.6	6.8 ± 0.9	5.6 ± 0.4	
	T_{CH}	0.3 ± 0.08	0.3 ± 0.06	0.5 ± 0.04	0.4 ± 0.09	0.4 ± 0.02	
	$T_{1\rho}$	9.3 ± 3.6	12.0 ± 4.2	6.6 ± 0.7	5.1 ± 1.1	6.0 ± 0.4	
E204Q	T_2	7.9 ± 1.3	6.4 ± 0.7	12.9 ± 2.3	7.8 ± 3.5	7.3 ± 1.2	
	T_{CH}	0.2 ± 0.03	0.4 ± 0.08	0.4 ± 0.08	0.3 ± 0.03	0.2 ± 0.05	
	$T_{1\rho}$	6.8 ± 0.9	4.4 ± 0.9	5.7 ± 1.1	7.4 ± .09	7.1 ± 1.7	

Conformational changes along the cytoplasmic half channel

The present finding of a significant displacement of the peptide bond of Val 49 in the D85N mutant indicates that there is the long-distance effect on backbone conformation between Asp 85 and Val 49 (Fig. 1). This finding implies that the protonation of Asp 85 in the photocycle will result in a local conformational change at Val 49 (Yamazaki et al., 1996). Fig. 6 demonstrates that the Val 49 ^{13}C chemical shift in the T46V mutant is displaced downfield by 0.15 ppm relative to that of the wild-type. In the x-ray diffraction structure (Luecke et al., 1998; Essen et al., 1998), however, no atoms of V49 and T46 are closer than 4 Å. The long-distance effect on backbone conformation must be indirect, i.e., by means other than the hydrogen bonds proposed by Yamazaki et al. (1996). It might have been expected that the Val 49 ^{13}C NMR signal would also be indirectly modified in the D96N mutant, in view of the interaction of the side-chains of Asp 96 and Thr 46 (Luecke et al., 1998; Essen et al., 1998). We found, however, no such displacement of the Val 49 peak (Fig. 6, *B* and *F*). It may be that the amide group of Asn 96 forms a hydrogen bond with Thr 46 in D96N, like the carboxyl group of Asp 96 in the wild-type.

A significant spectral change occurs in either Val 69 or 101, or both, however, upon replacement of Asp 96 with Asn. It is likely that the new peak at 173.52 ppm that appears in D96N is to be ascribed to Val 101 because of its proximity to Asp 96.

It is notable that the T_2 values for Val 199 are substantially decreased in a variety of mutants as compared with wild-type (Table 1). In particular, the observed shortened T_2 value of Val 199 in the D96N mutant indicates that there is interaction between Asp 96 and the backbone near the extracellular surface at Val 199. This interaction must be transmitted across the protein in the T46-V49-D85-E204 domain, through the conformational interactions between Thr 46 and Val 49, Val 49 and Asp 85, and Asp 85 and Glu 204, described above and in the following section.

Conformational changes induced near the extracellular surface

We found that the Val 49 signal is also displaced in the E204Q mutant, although the direction of the displacement in this case is opposite to that of D85N. This finding suggests interaction between Glu 204 and Val 49 mediated by Asp 85. This would be consistent with the finding that the pK_a values of Asp 85 and Glu 204 are coupled to each other (Richter et al., 1996; Balashov et al., 1997). In addition, we found evidence of interaction between Asp 85 and Glu 194 and 204 through Arg 82, as manifested from the induced conformational change at the extracellular surface on the basis of spectral changes in the ^{13}C NMR spectrum of [3-^{13}C]Ala-D85N, which parallel those in E194D, E194Q, and E204Q (M. Tanio, S. Tuzi, S. Yamaguchi, R. Kawaminami, A. Naito, R. Needleman, J. K. Lanyi, and H. Saitô, submitted for publication). The effects of mutations on the ^{13}C chemical shifts of Val 199 in the F-G loop are in the same direction for D85N and E204Q. This effect is less pronounced than for Val 49, suggesting that the interaction with Asp 85 might be stronger with Val 49 than with Val 199. It was reported earlier from photocycle kinetics (Brown et al., 1994b) that the pK_a difference between the retinal Schiff base and Asp 85 changed when the side chain of residue 49 was changed. Thus, the interaction of Val 49 with Asp 85 could be mediated by the intervening Schiff base. It is interesting to note also that in the recent x-ray diffraction structure of Luecke et al. (1998), Asp 85 is connected with Glu 204 through a hydrogen-bonded network of two water molecules, the retinal Schiff base, Asp 212 and Arg 82. It may be expected from this structure that disruption or perturbation of this network would bring about a conformational change.

CONCLUSION

Studies of the displaced ^{13}C chemical shifts of [1-^{13}C]Val-labeled unphotolyzed wild-type and mutants are novel means to analyze snapshots of local interactions among molecular chains that arise from conformational changes. In particular, the dynamic features of the local conformations can readily be evaluated by examination of the relaxation parameters at ambient temperature. This sort of information is important, because these molecular processes occur at physiological temperature and could mimic what happens during the photocycle of bR.

In particular, the data for the T46V mutant indicate that there is a specific interaction between hydroxyl group of Thr 46 and carbonyl or amide of Val 49, which are only about one helix turn apart. Further, the results with D85N and E204Q show that there exist interactions between Val 49 and Asp 85 and between Asp 85 and Glu 204, respectively. Therefore, we conclude that there exists an interacting chain of residues and backbone that comprise T46-V49-D85-E204. In addition, the present finding based on the T_2 measurement indicates that there exists interaction between Asp 96 and extracellular surface, probably through the above-mentioned interacting chain. The long-distance effect on backbone conformation is through a hydrogen-bonded chain in the extracellular region, but its nature in the cytoplasmic region is not yet clear. The findings from NMR thus confirm the conclusions made from FTIR (Yamazaki et al., 1995, 1996, 1998), and suggest that protonation of Asp 85 during the photocycle might induce changed conformation and/or dynamics at both the extracellular surface and side chain of Asp 96. This kind of long-range interaction could be relevant in general also to signal transduction systems such as G-protein coupled or other receptor molecules.

This work was supported in part by grants-in-aid for the Scientific Research from the Ministry of Education, Science, Culture and Sports in Japan (09480179 and 10044092) and a special grant from Hyogo Prefecture.

REFERENCES

Balashov, S. P., E. S. Imasheva, T. G. Ebrey, N. Chen, D. R. Menick, and R. K. Crouch. 1997. Glutamate-194 to cysteine mutation inhibits fast light-induced proton release in bacteriorhodopsin. *Biochemistry.* 36: 8671–8676.

Brown L. S., Y. Yamazaki, A. Maeda, L. Sun, R. Needleman, and J. K. Lanyi. 1994a. The proton transfers in the cytoplasmic domain of bacteriorhodopsin are facilitated by a cluster of interacting residues. *J. Mol. Biol.* 239:401–414.

Brown, L. S., Y. Gat, M. Sheves, Y. Yamazaki, A. Maeda, R. Needleman, and J. K. Lanyi. 1994b. The retinal Schiff base-counterion complex of bacteriorhodopsin: changed geometry during the photocycle is a cause of proton transfer to aspartate 85. *Biochemistry.* 33:12001–12011.

Brown, L. S., J. Sasaki, H. Kandori, A. Maeda, R. Needleman, and J. K. Lanyi. 1995. Glutamic acid 204 is the terminal proton release group at the extracellular surface of bacteriorhodopsin. *J. Biol. Chem.* 270: 27122–27126.

Dioumaev, A. K., H. T. Richter, L. S. Brown, M. Tanio, S. Tuzi, H. Saitô, Y. Kimura, R. Needleman, and Lanyi, J. K. 1998. Existence of a proton transfer chain in bacteriorhodopsin: participation of Glu-194 in the release of protons to the extracellular surface. *Biochemistry.* 37: 2496–2506.

Engelhard, M., S. Finkler, G. Metz., and F. Siebert. 1996. Solid-state ^{13}C-NMR of [(3-^{13}C)Pro]bacteriorhodopsin and [(4- ^{13}C)Pro] bacteriorhodopsin: evidence for a flexible segment of the C- terminal tail. *Eur. J. Biochem.* 235:526–533.

Engelhard, M., B. Hess, D. Emeis, G. Metz, W. Kreutz, and F. Siebert. 1989. Magic angle sample spinning ^{13}C nuclear magnetic resonance of isotopically labeled bacteriorhodopsin. *Biochemistry.* 28:3967–3975.

Essen, L., R. Siegert, W. D. Lehmann, and D. Oesterhelt. 1998. Lipid patches in membrane protein oligomers: crystal structure of the bacteriorhodopsin-lipid complex. *Proc. Natl. Acad. Sci. USA.* 95: 11673–11678.

Govindjee, R., S. Misra, S. P. Balashov, T. G. Ebrey, R. K. Crouch, and D. R. Menick. 1996. Arginine-82 regulates the pK_a of the group responsible for the light- driven proton release in bacteriorhodopsin. *Biophys. J.* 71:1011–1023.

Grigorieff, N., T. A. Ceska, K. H. Downing, J. M. Baldwin, and R. Henderson. 1996. Electron-crystallographic refinement of the structure of bacteriorhodopsin. *J. Mol. Biol.* 259:393–421.

Howarth, O. W., and D. M. J. Lilley. 1978., Carbon-13-NMR of Peptides and Proteins. *Prog. NMR Spectrosc.* 12:1–40.

Henderson, R., J. M. Baldwin, T. A. Ceska, F. Zemlin, E. Beckmann, and K. H. Downing. 1990. Model for the structure of bacteriorhodopsin based on high-resolution electron cryo-microscopy. *J. Mol. Biol.* 213: 899–929.

Hu, J. G., B. Q. Sun, M. Bizounok, M. E. Hatcher, J. C. Lansing, J. Raap, P. J. Verdegem, J. Lugtenburg, R. G. Griffin, and J. Herzfeld. 1998. Early and late M intermediates in the bacteriorhodopsin photocycle: a solid-state NMR study. *Biochemistry.* 37:8088–8096.

Kataoka, M., K. Mihara, H. Kamikubo, R. Needleman, J. K. Lanyi, and F. Tokunaga. 1993. Trimeric mutant bacteriorhodopsin, D85N, shows a monomeric CD spectra. *FEBS Lett.* 333:111–113.

Kimura, Y., D. G. Vassylyev, A. Miyazawa, A. Kidera, M. Matsushima, K. Mitsuoka, K. Murata, T. Hirai, and Y. Fujiyoshi. 1997. Surface of bacteriorhodopsin revealed by high-resolution electron crystallography. *Nature.* 389:206–211.

Lanyi, J. K. 1993. Proton translocation mechanism and energetics in the light-driven pump bacteriorhodopsin. *Biochim. Biophys. Acta.* 1183: 241–246.

Lanyi, J. K. 1997. Mechanism of ion transport across membranes. Bacteriorhodopsin as a prototype for proton pumps. *J. Biol. Chem.* 272: 31209–31212.

Luecke, H., H. T. Richter, and J. K. Lanyi. 1998. Proton transfer pathways in bacteriorhodopsin at 2.3 angstrom resolution. *Science.* 280: 1934–1937.

Maeda, A., H. Kandori, Y. Yamazaki, S. Nishimura, M. Hatanaka, Y. S. Chon, J. Sasaki, R. Needleman, and J. K. Lanyi. 1997. Intramembrane signaling mediated by hydrogen-bonding of water and carboxyl groups in bacteriorhodopsin and rhodopsin. *J. Biochem. (Tokyo).* 121:399–406.

Mathies, R. A., S. W. Lin, J. B. Ames, and W. T. Pollard. 1991. From femtoseconds to biology: mechanism of bacteriorhodopsin's light-driven proton pump. *Annu. Rev. Biophys. Chem.* 20:491–518.

Metz, G., F. Siebert, and M. Engelhard. 1992a. Asp85 is the only internal aspartic acid that gets protonated in the M intermediate and the purple-to-blue transition of bacteriorhodopsin. A solid-state ^{13}C CP-MAS NMR investigation. *FEBS Lett.* 303:237–241.

Metz, G., F. Siebert, and M. Engelhard. 1992b. High-resolution solid state ^{13}C NMR of bacteriorhodopsin: characterization of [4-^{13}C]Asp resonances. *Biochemistry.* 31:455–462.

Naito, A., A. Fukutani, M. Uitdehaag, S. Tuzi, and H. Saitô. 1998. Backbone dynamics of polycrystalline peptides studied by measurements of ^{15}N NMR lineshapes and ^{13}C transverse relaxation times. *J. Mol. Struct.* 441:231–241.

Oesterhelt, D., and W. Stoeckenius. 1974. Isolation of the cell membrane of Halobacterium halobium and its fractionation into red and purple membrane. *Methods Enzymol.* 31:667–678.

Onishi, H., E. McCance, and N. E. Gibbons. 1965. A synthetic medium for extremely halophilic bacteria. *Can. J. Microbiol.* 11:365–373.

Pebay-Peyroula, P. E., G. Rummel, J. P. Rosenbusch, and E. M. Landau. 1997. X-ray structure of bacteriorhodopsin at 2.5 angstroms from microcrystals grown in lipidic cubic phases. *Science.* 277:1676–1681.

Pervushin K. V., V. Y. Orekhov, A. I. Popov, L. Y. Musina, and A. S. Arseniev. 1994. Backbone dynamics of (1–27)bacteriorhodopsin studied by two-dimensional ^{1}H-^{15}N NMR spectroscopy. *Eur. J. Biochem.* 219: 571–583.

Popot, J.-L., S.-E. Gerchman, and D. M. Engelman, 1987. Refolding of bacteriorhodopsin in lipid bilayers. A thermodynamically controlled two-stage process. *J. Mol. Biol.* 198:655–676.

Rammelsberg, R., G. Huhn, M. Lubben, and K. Gerwert. 1998. Bacteriorhodopsin's intramolecular proton-release pathway consists of a hydrogen-bonded network. *Biochemistry.* 37:5001–5009.

Richter, H. T., L. S. Brown, R. Needleman, and J. K. Lanyi. 1996. A linkage of the pK_a's of asp-85 and glu-204 forms part of the reprotonation switch of bacteriorhodopsin. *Biochemistry.* 35:4054–4062.

Rothwell, W. P., and J. S. Waugh. 1981. Transverse relaxation of dipolar coupled spin systems under rf irradiation: Detecting motions in solid. *J. Chem. Phys.* 75:2721–2732.

Saitô, H. 1986. Conformation-dependent ^{13}C chemical shifts: a new means of conformational characterization as obtained by high-resolution solid-state NMR. *Magn. Reson. Chem.* 24:835–852.

Saitô, H., and I. Ando. 1989. High-resolution solid-state NMR studies of synthetic and biological macromolecules. *Annu. Rep. NMR Spectrosc.* 21:209–290.

Saitô, H., S. Tuzi, and A. Naito. 1998. Empirical versus nonempirical evaluation of secondary structure of fibrous and membrane protein by solid-state NMR: a practical approach. *Annu. Rep. NMR Spectrosc.* 36:79–121.

Stoeckenius, W., and R. A. Bogomolni. 1982. Bacteriorhodopsin and related pigments of halobacteria. *Annu. Rev. Biochem.* 52:587–616.

Suwelack, D., W. P. Rothwell, and J. S. Waugh. 1980. Slow molecular motion detected in the NMR spectra of rotating solids. *J. Chem. Phys.* 73:2559–2569.

Tanio, M., S. Tuzi, S. Yamaguchi, H. Konishi, A. Naito, R. Needleman, J. K. Lanyi, and H. Saitô. 1998. Evidence of local conformational fluctuations and changes in bacteriorhodopsin, dependent on lipids, detergents and trimeric structure, as studied by ^{13}C NMR. *Biochim. Biophys. Acta.* 1375:84–92.

Torchia, D. A. 1978. The measurement of proton-enhanced carbon-13 T_1 values by a method which suppresses artifacts. *J. Magn. Reson.* 30: 613–616.

Torchia, D. A., and J. R. Lyerla, Jr. 1974. Molecular mobility of polypeptides containing proline as determined by ^{13}C magnetic resonance. *Biopolymers.* 13:97–114.

Tuzi, S., A. Naito, and H. Saitô. 1993. A high-resolution solid-state ^{13}C-NMR study on [1-^{13}C]Ala and [3-^{13}C]Ala and [1-^{13}C]Leu and Val-labelled bacteriorhodopsin. *Eur. J. Biochem.* 218:837–844.

Tuzi, S., A. Naito, and H. Saitô. 1994. ^{13}C NMR study on conformation and dynamics of the transmembrane α helices, loops, and C-terminus of [3-^{13}C]Ala-labeled bacteriorhodopsin. *Biochemistry.* 33:15046–15052.

Tuzi, S., A. Naito, and H. Saitô. 1996a. Temperature-dependent conformational change of bacteriorhodopsin as studied by solid-state ^{13}C NMR. *Eur. J. Biochem.* 239:294–301.

Tuzi, S., S. Yamaguchi, A. Naito, R. Needleman, J. K. Lanyi, and H. Saitô. 1996b. Conformation and dynamics of [3-^{13}C]Ala- labeled bacteriorhodopsin and bacterioopsin, induced by interaction with retinal and its analogs, as studied by ^{13}C nuclear magnetic resonance. *Biochemistry.* 35:7520–7527.

Tuzi, S., S. Yamaguchi, M. Tanio, H. Konishi, S. Inoue, A. Naito, R. Needleman, J. K. Lanyi, and H. Saitô. 1999. Location of a cation binding site in the loop between helices F and G of bacteriorhodopsin, as studied by ^{13}C NMR. *Biophys. J.* 76:1523–1531.

Wikström, M. 1998. Proton translocation by bacteriorhodopsin and heme-copper oxidases. *Curr. Opin. Struct. Biol.* 8:480–488.

Wishart, D. S., B. D. Sykes, and F. M. Richards. 1991. Relationship between nuclear magnetic resonance chemical shift and protein secondary structure. *J. Mol. Biol.* 222:311–333.

Wishart, D. S., C. G. Bigam, A. Holm, R. S. Hodges, and B. D. Sykes. 1995. ^{1}H, ^{13}C, and ^{15}N random coil NMR chemical shifts of the common amino acids. I. Investigations of nearest-neighbor effects. *J. Biomol. NMR.* 5:67–81.

Yamaguchi, S., S. Tuzi, T. Seki, M. Tanio, R. Needleman, J. K. Lanyi, A. Naito, and H. Saitô. 1998. Stability of the C-terminal α-helical domain of bacteriorhodopsin that protrudes from the membrane surface, as studied by high-resolution solid-state ^{13}C NMR. *J. Biochem. (Tokyo).* 123:78–86.

Yamazaki, Y., M. Hatanaka, H. Kandori, J. Sasaki, W. F. Karstens, J. Raap, J. Lugtenburg, M. Bizounok, J. Herzfeld, R. Needleman, J. K. Lanyi, and A. Maeda. 1995. Water structural changes at the proton uptake site (the Thr46-Asp96 domain) in the L intermediate of bacteriorhodopsin. *Biochemistry.* 34:7088–7093.

Yamazaki, Y., S. Tuzi, H. Saitô, H. Kandori, R. Needleman, J. K. Lanyi, and A. Maeda. 1996. Hydrogen bonds of water and C = O groups coordinate long-range structural changes in the L photointermediate of bacteriorhodopsin. *Biochemistry.* 35:4063–4068.

Yamazaki, Y., H. Kandori, R. Needleman, J. K. Lanyi, and A. Maeda. 1998. Interaction of the protonated Schiff base with the peptide backbone of valine 49 and the intervening water molecule in the N photointermediate of bacteriorhodopsin. *Biochemistry.* 37:1559–1564.